ORIGINAL ARTICLE

Thioimidazolate versus pyrazolate-zinc(II)-bound hydroxo complex as structural model for the active site of hydrolytic enzyme: the crystal structure of the inclusion complex TtZn–O–C$_6$H$_4$–p-NO$_2$, Tt = hydrotris(N-xylyl-2-thioimidazolyl)borate

Mohamed M. Ibrahim · Abd El-Motaleb. M. Ramadan

Abstract The reaction of the tripod ligand hydrotris(N-(2-methylphenyl)-2-thioimidazol-1-yl)borate, **Tt** with zinc(II) chloride yielded the chloro complex [**Tt**Zn–Cl] **1**. The hydrolytic reactivity of its hydroxo complex [**Tt**Zn–(μ-OH)Zn**Tt**]Cl **2** towards p-nitrophenyl acetate was hampered due to the formation of the stable phenolate complex [**Tt**Zn–O–Ar–p-NO$_2$] **3** as a product inhibition. The X-ray structure analysis of complex **3** was determined and showed that its Zn[S$_3$O] coordination sphere includes three thione donors from the ligand **Tt** and one oxygen donor from the hydrolysed product p-nitrophenolate in an ideally tetrahedral arrangement around the zinc(II) centre.

Keywords Thioimidazolylborate · Zinc(II) complexes · Crystal structure · Carboxyester hydrolysis

Introduction

Since the nature of donor ligand is a commonly employed technique of providing both structural and mechanistic information [1–6], it is important to ascertain how biologically relevant ligand complements influence the hydrolytic activity of zinc model complexes.

M. M. Ibrahim (✉) · A. E.-M. M. Ramadan
Chemistry Department, Faculty of Science, Kafr El-Sheikh University, Kafr El-Sheikh 33516, Egypt
e-mail: ibrahim652001@yahoo.com

M. M. Ibrahim
Chemistry Department, Faculty of Science, Taif University, Taif 888, Saudi Arabia

The properties of the tripod ligands, containing the three heterocyclic rings tris(thioimidazolyl)borate **Tt^R** [7] suggests that it can form four-coordinate zinc(II) complexes with additional ligation from one exogenous neutral or anionic ligand, e.g., [**Tt**Zn–X]$^+$ (X = H$_2$O or ROH) [4], [**Tt^R**Zn–X] (X = OH, OR or SR) [8–17]. These zinc(II) model complexes have provided important information concerning the structure and the mechanism of (Cys)$_3$Zn(II) proteins such as *alcohol dehydrogenase* and *Ada repair protein* [18].

As a part of our studies in mimicking the zinc(II) coordination structure as well as the function of the zinc(II) ion at the active site of non-redox enzymes, several mononuclear zinc(II) complexes were designed and investigated to elucidate the detailed reaction mechanism in these hydrolytic zinc enzymes [19–32]. Using this approach, the influence of ligating S$_3$ donor set on the hydrolysis of p-nitrophenyl acetate in tripod zinc(II) complexes was studied. The crystal structure of the inclusion complex containing the hydrolyzed product, **Tt**Zn–OC$_6$H$_4$–p-NO$_2$ **3** was also reported.

Experimental

General data

temperature with a germanium detector, maintained at liquid nitrogen temperature and using 1064.0 nm radiation, generated by a Nd-YAG laser with a resolution of 2 cm^{-1}. The samples were exposed to an average of 500–800 mW of laser intensity during the spectral recording. ^{1}H NMR spectra were measured on a JEOL EX-400 instrument. The chemical shifts are reported relative to the resonance signal of the tetramethyl silane (TMS) as an internal standard signal. The electrical molar conductivity measurements were carried out using Equiptronics digital conductivity meter model JENWAY 4070 type at room temperature for $(1 \times 10^{-3}$ M) solutions. All UV–Visible measurements were recorded by UV-1650pc Shimadzu.

Synthesis

Hydrotris[N-(2-methylphenyl)-2-thioimidazol-1-yl)boratochlorozinc

A solution of 185 mg (0.3 mmol) of **Tt** in abs. MeOH (10 mL) was added dropwise (30 min) to the methanolic solution of 41 mg (0.3 mmol) of $ZnCl_2$. The reaction mixture was stirred for 2 h at room temperature, and then the solvent was evaporated to dry. The residue was dissolved in 10 mL of CH_2Cl_2, which was filtered off, and then evaporated to dry again to give a white powder. Yield 164 mg (81%); m.p. 214 °C (dec). Anal. For $C_{30}H_{28}BClN_6S_3Zn$ [**Tt**Zn–Cl]: IR (KBr): v (cm^{-1}): 3430 (br, w), 3166 (w), 3137 (w), 2448 (w, B–H), 1620 (w), 1560 (w), 1498 (s), 1462 (m), 1426 (m), 1373 (s), 1321 (w), 1302 (w), 1041 (w), 1018 (m), 957 (w), 890 (w), 770 (m), 739 (m), 717 (w), 690 (w), 672 (w), 623 (w).

μ-Hydroxo-[bis{hydrotris(N-(2-methylphenyl)-2-thioimidazol-1-yl)borate-zinc}]chloride

A solution of 185 mg (0.3 mmol) of **Tt** in abs. MeOH (10 mL) was added dropwise (30 min) to a solution of 41 mg (0.3 mmol) of $ZnCl_2$ dissolved in abs. MeOH (10 mL). The resulting reaction mixture was stirred for 2 h at room temperature. The liberated KCl salt was removed from the reaction mixture by filtration and then a solution of 17 mg (0.3 mmol) of KOH in abs. MeOH (5 mL) was added with constant stirring. The reaction mixture was further stirred for another 15 h at room temperature to form white precipitate. The final product (hydroxo complex) was extracted by using CH_2Cl_2, which was further filtered off and finally evaporated to dry again to give white powder. Single crystal suitable for X-ray crystallography was obtained from MeOH:CH_2Cl_2 mixture. Yield 297 mg (74%); m.p. 234 °C (dec). Anal. For $C_{60}H_{57}B_2ClN_{12}$

OS_6Zn_2 ([**Tt**Zn(μ-OH)Zn**Tt**]Cl·CH$_3$OH): IR (KBr): v (cm^{-1}): 3508 (br, w), 3165 (m), 3132(m), 3092 (m), 3035 (m), 2970 (m), 2920 (m), 2856 (m), 2442, 2418 (w, B–H), 1603 (m), 1560 (m), 1479 (s), 1444 (m), 1420 (m), 1372 (s), 1310 (s), 1243 (s), 1190 (s), 1045 (m), 984 (m), 953 (m), 781 (s), 746 (m), 693 (m), 623 (m), 583 (m), 521 (m), 502 (m).

Hydrotris[N-(2-methylphenyl)-2-thioimidazol-1-yl]borato-p-nitrophenolato-zinc

A solution of 185 mg (0.3 mmol) of **Tt** in abs. MeOH (10 mL) was added dropwise (30 min) to a solution of 112 mg (0.3 mmol) of $Zn(ClO_4)_2$·6H$_2$O dissolved in abs. MeOH (10 mL). The reaction mixture was stirred for 2 h at room temperature and then it was filtered off to isolate the inorganic salt $KClO_4$. A solution of 44 mg (0.3 mmol) of KOArNO$_2$ in abs. MeOH (10 mL) was added to the reaction mixture and the formed yellow solution was stirred for another 8 h at room temperature. The solvent was removed under vacuum at 40 °C and the resulting zinc(II) complex was extracted with CH_2Cl_2, which was evaporated to dry again to yield the microcrystalline powder complex **3**. The single yellow crystal suitable for X-ray measurement was obtained from methanol:dichloromethane mixture. Yield 180 mg (77%); m.p. 226 °C (dec.). IR (KBr): v (cm^{-1}): 3442 (br, w), 3126 (w), 2442 (w, B–H), 1582 (m), 1498 (m), 1464 (w), 1426 (w), 1371 (m), 1297 (s), 1186 (m), 1109 (w), 995 (w), 955 (w), 849 (w), 826 (w), 803 (w), 716 (m), 690 (w), 654 (w).

X-ray single crystal determination of complex **3**

Crystals of **3** were obtained by recrystallisation from methanol:dichloromethane (3:1). The crystallographic data were collected on a Smart-CCD diffractometer of Bruker AXS using Mo Ka radiation. None of the crystals show significant intensity loss throughout the data collections. Lorentz-polarization corrections were performed by SAINT [33]. Absorption corrections were made by using the SADABS program [34]. The structures were solved by direct or Patterson methods using SHELXS-97 [35] to find out the position of the heavy atoms. The other non-hydrogen atoms were located by Fourier syntheses and refined using SHELXS-97 [12]. The least squares refinements were performed using all independent reflections by the full matrix on F2. The hydrogen atoms were positioned at calculated sites (with C–H 0.96 Å) and were constrained to ride on their linked atoms with isotropic thermal parameters of 1.5 times the factor of the methyl groups and 1.2 times the factor of the other groups. Table 1 lists the crystallographic details.

Table 1 Crystal data and structure refinement of **Tt**Zn-O–Ar–*p*-NO$_2$ **3**

	3 0.5 CH$_3$OH
Empirical formula	C$_{150}$H$_{144}$B$_4$Cl$_8$N$_{28}$O$_{14}$S$_{12}$Zn$_4$
Formula weight	3535.97
Crystal size (mm)	0.10 × 0.20 × 0.27
Crystal colour	Colorless
Space group	*P-1*
Z	2
a (Å)	13.841(3)
b (Å)	18.703(3)
c (Å)	31.752(6)
α (°)	89.999(3)
β (°)	89.978(3)
γ (°)	80.481(3)
Volume (Å^3)	8106(3)
d (calc.) (g cm^{-3})	1.449
μ(Mo Kα) (mm^{-1})	0.940
Temperature (K)	506(2)
Θ-range (°)	1.10–29.06
Index ranges	$-17 \leq h \leq 17, -24 \leq k \leq 25, -43 \leq l \leq 41$
Absorption correction	SADABS
Reflections collected	74026
Independent reflections	38176[*R*(int) = 0.1663]
Refelctions observed [$I > 2\sigma(I)$]	8038
Data	38176
Parameters	1983
Goodness-of-fit	0.851
Final *R* indices [$I > 2\sigma(I)$]	$R_1 = 0.0985, wR_2 = 0.2471$
R indices (all data)	$R_1 = 0.3319, wR_2 = 0.3514$
Largest diff. peak [e.Å^{-3}]	1.090
And hole	−1.048

Kinetic studies for the hydration reaction
of *p*-nitrophenyl acetate

The rate of catalytic hydrolysis of *p*-nitrophenyl acetate, NA in chloroform by using the hydroxo complex **2** was measured by recording the increase in 384 nm absorption of the generated *p*-nitrophenoxide complex **4** as hydrolysis product. The measurements of the hydrolysis reactions were carried out at 25.0 ± 0.2 °C. The measurements were carried out at 300 K. Reactions were carried out under pseudo-first order conditions by adding 50 µL of a 5 mM solution of NA (ca. 8×10^{-5} mM initial concentration) in acetonitrile solution to the spectrophotometer cell (total volume 3 mL) containing different concentrations of **2** (0.5–2.5 mM). The first order rate constants were estimated from the integrated form of the first order low and the

second-order rate constant was calculated from the slope of k_{obs} versus concentration of zinc complex **2**.

Results and discussion

Characterization of zinc(II) complexes

Zinc(II) complexes of the tripod tris(thioimidazolyl)borate have been thoroughly reviewed by Parkin [5]. Recently we [7–17] have prepared a series of thione–thiolate zinc(II) complexes, crystal structure analysis and detailed NMR studies were reported. The tripod ligand **Tt** [36] was used to emulate the [S$_3$] coordination environment provided by the three cysteine protein residues in zinc enzymes. The four coordinated chloro complex [**Tt**Zn–Cl] **1** was prepared in a high yield by treating the potassium salt of the ligand with an equimolar amount of ZnCl$_2$ in absolute methanol. The resulting zinc complex **1** was isolated by extraction using CH$_2$Cl$_2$ as an extracting solvent and the final product was purified by crystallization from methanol:dichloromethane mixture. Treatment of complex **1** with the deprotonated form of *p*-nitrophenol leads to the formation of the yellow **Tt**Zn-bound *p*-nitrophenolate complex **3**. Single crystal suitable for X-ray measurements was grown from MeOH:CH$_2$Cl$_2$.

The important infrared spectral bands in the 4000–400 cm^{-1} region of the ligand **Tt** and its zinc(II) complexes [**Tt**Zn–Cl] **1** and [**Tt**Zn–OAr–*p*-NO$_2$] **3** are shown in Fig. 1. Several main spectral features should be noted. The v(B–H) absorption band of zinc(II) complex **1** at 2448 cm^{-1} and **3** at 2442 cm^{-1} was shifted around
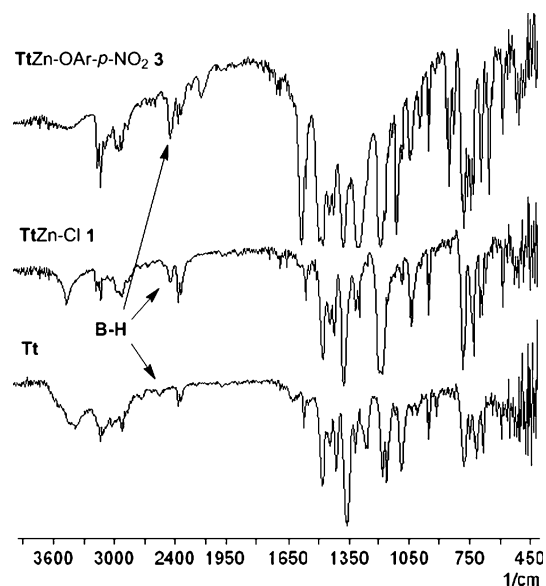

Fig. 1 FT-IR spectra of the ligand **Tt**, zinc(II) complex **1**, and zinc(II) complex **3**
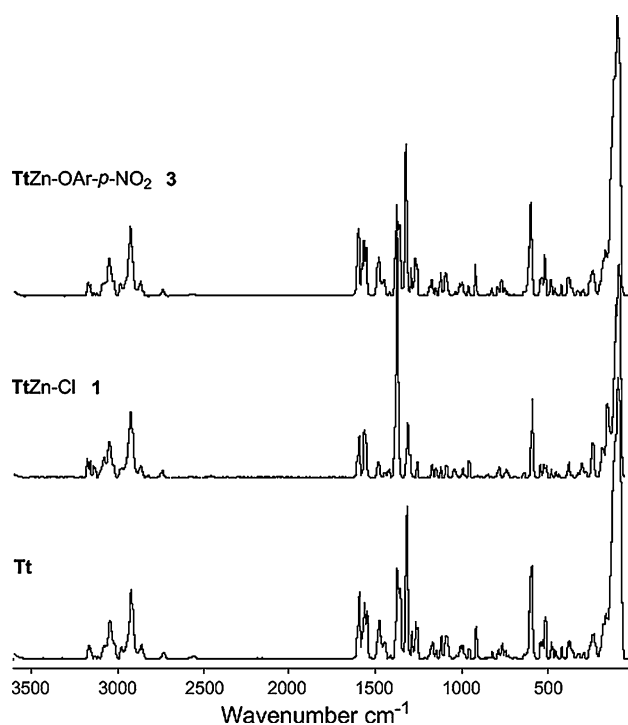
Fig. 2 Raman spectra of the ligand **Tt**, zinc(II) complex **1**, and zinc(II) complex **3**

$100 \, cm^{-1}$ to lower energy relative to that of the free ligand. In all these complexes the presence of two very intense bands at 1059 and 1039 cm^{-1} was assigned as C=S terminal stretching. These bands are generally used to confirm the presence of **Tt** ligand in all complexes. Other assignments are: bands at 995 and 887 cm^{-1} to C–S stretches, the low intensity band at 524 cm^{-1}, a breathing mode of the heterocycle **Tt** complex, and the bands below 500 cm^{-1}, to angular deformation and Zn–S stretching modes. These shifts may result from changes in the electronic state where the C=S bond loses some of its double bond character when the ligand coordinates via the thione sulfur. The shifts in the bands between the free ligand and the complexes result from electronic shifts within the ligand.

Information about the low frequency zinc(II)–chloride and zinc(II)–S(thionate) vibrations can be obtained by using Raman spectroscopy. Typical Raman spectra obtained for the the ligand **Tt** and its zinc(II) complexes **1**

and **3** are shown in Fig. 2. The bands of most interest are the ones formed upon complexation, which must therefore be the result of zinc(II)–chlorine bonding or zinc(II)–S/O bonding. In the spectra shown, prominent new bands include the strong peaks around 248 and 175 cm^{-1} for the 1:1 complex with the ligand **Tt**, which we conclude that the result of the formation of zinc(II)–ligand bonds through the sulfur atom. The Zn(II)–Cl band in **1**, on the other hand, does not occur in the same position for all of the complexes, due to the different mass of the chlorine atom and the different bond strengths upon complexation. The Raman data for the complexes show bands are formed upon complexation that is common to all the 1:1 at 285 cm^{-1}. The Zn(II)–Cl vibrations can clearly be identified at 248 cm^{-1}.

The molar conductivity measurements of the reported complexes in DMSO (Table 2) show that the chloride anion for complex **1** and the *p*-nitrophenolate anion in the case of complex **3** are coordinated to the zinc centers. The conductance values lie in the range acceptable for a 1:1 eletrolyte. Complementary information is obtained by assignment of ^{1}H and ^{13}C spectral features of the ligand and its complexes **1** and **3** in CDCl$_3$ (Table 3). The ^{1}H NMR signals of the thioimidazolyl and phenyl protons of complex **1** and **3** are shifted downfield compared to their positions in the spectra of the free ligand, suggesting that in CDCl$_3$ the ligand signals remain coordinated to zinc(II) ions. The ^{13}C band assignments showed that the carbon atom (C(2)) attached to the thione sulfur clearly shows the greatest chemical shift, up to ~6 ppm from the free ligand. This finding reflects that this band is thus the most sensitive to coordination. The ethylenic carbons (C(4), C(5)) show much smaller chemical shifts, thus coordination in all complexes must be via the thione sulfur atom. These results confirm that, in the solid state the coordination of the ligand takes place only through the sulfur atom only [7–17]. The most characteristic feature of complex **3** in ^{1}H NMR spectrum is the appearance of the two doublets at 6.44 and 7.81 ppm, which were assigned to the proton resonances of the coordinated *p*-nitrophenolate.

Treatment of zinc(II) complex **1** with KOH in anhydrous methanol under anaerobic conditions afforded the bridged hydroxide complex [**TtZn–(μ-OH)ZnTt**]Cl **2** as crystalline

Table 2 Physical and analytical data of zinc(II) complexes **1–3**

Complex	Found (calc.)%					Λ_m (Ω cm, mole^{-1})
	%C	%H	%N	%S	%Cl	
1	52.08 (52.96)	4.31 (4.15)	12.44 (12.35)	14.01 (14.14)	10.12 (5.21)	39
2	54.54 (53.31)	4.23 (4.36)	12.23 (12.11)	14.00 (13.81)	2.58 (2.66)	119
3	50.92 (50.71)	4.38 (4.26)	10.77 (10.89)	10.71 (10.69)	–	34

Table 3 ^{1}H–^{13}C NMR spectral data of the ligand **Tt** and its zinc(II) complexes **1–3**
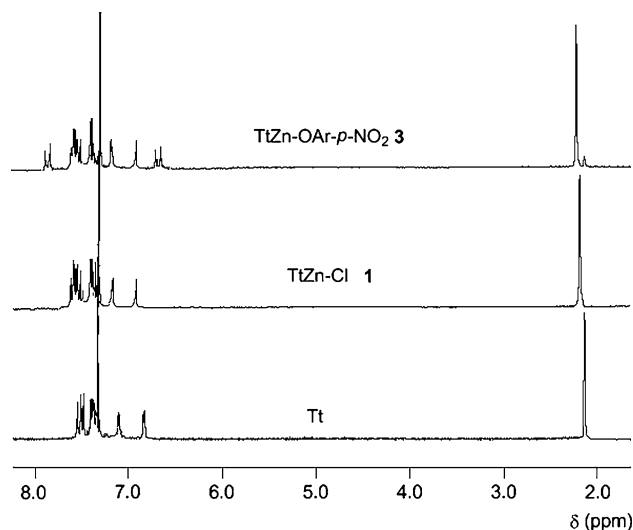
Comp.	$\delta(-CH_3)$		$\delta(-C^1)$	$\delta(-C^2H)$		$\delta(-C^3H)$		$\delta(-Aryl)$		$\delta(-C_6H_4-p-NO_2)$		
	^{1}H	^{13}C	^{13}C	^{1}H	^{13}C	^{1}H	^{13}C	^{1}H	^{13}C	^{1}H		^{13}C
Tt[a]	1.95 (s, 9H)	19.2	166.5	6.89 (d, 3H)	114.3	6.71 (d, 3H)	111.9	7.20–7.35 (m, 12H)	122.9, 123.5, 126.8 131.1, 135.9, 136.7			
1	2.13 (s, 9H)	24.7	171.2	6.96 (d, 3H)	115.5	7.16 (d, 3H)	113.6	7.22–7.37 (m, 12H)	124.5, 126.2, 127.9 133.0, 138.9, 137.9			
2	1.93 (s, 18H)	22.1	168.3	6.51 (d, $^3J = 2.1$, 6H)	113.1	6.75 (d, $^3J = 2.1$, 6H)	112.9	7.13–7.22 (m, 24H)	123.1, 124.8, 126.6 131.2, 137.7, 136.8			
3	2.11 (s, 18H)	24.4	170.4	6.97 (d, $^3J = 2.2$, 3H)	114.9	7.16 (d, $^3J = 2.2$, 6H)	113.8	7.29–7.42 (m, 12H)	124.3, 125.9, 127.3 132.7, 138.4, 137.6	6.44 (d, $^3J = 9.01$ Hz, 2H, nitro (2,6))	7.81 (d, $^3J = 9.20$ Hz, 2H, Nitro (3,5))	118.3, 126.5, 141.6, 166.1

[a] ^{1}H NMR measurement of the ligand S_3 [35]

Table 4 Bond lengths (Å) and angles (°) of **TtZn–O–Ar–p-NO$_2$ 3**

Bond length (Å)	Zn(1)–O(1)	1.951(7)
	Zn(1)–S(2)	2.341(3)
	Zn(1)–S(3)	2.359(3)
	Zn(1)–S(1)	2.339(3)
Bond angles (°)	O(1)–Zn(1)–S(2)	117.4(2)
	O(1)–Zn(1)–S(3)	109.4(2)
	S(2)–Zn(1)–S(3)	106.55(11)
	O(1)–Zn(1)–S(1)	107.3(2)
	S(2)–Zn(1)–S(1)	108.10(11)
	S(3)–Zn(1)–S(1)	107.74(11)

Fig. 3 ^{1}H NMR spectra of the ligand **Tt** and its zinc complexes **1** and **3** in CDCl$_3$

solid with good yields. Its chemical characterisation was determined by ^{1}H NMR, IR, and mass spectroscopy. In freshly prepared methanol solutions positive ion elctrospray mass spectra (ESI-MS) on the zinc hydroxide species **2** shows two clean mass. The first has an m/e cenetered around 645 amu and an isotope pattern indicative of the mononuclear [**Tt**Zn]$^+$ cation. The second has centred about 1306 amu and an isotope pattern that is consistent with the [**Tt**Zn((μOH)Zn**Tt**]$^+$ cation. Thus the binuclear species represented by the solid state structure appears to maintain its integrity in solution. The formation of the bridged hydroxo complex **2** in comparison to the monomeric zinc hydroxide complex of the tris(pyrazolyl)borate, KTp ligand [37–39] suggests its high nucleophilicity and it has a great potential for altering the electron density at the zinc center and also the substituents attached to the thioimidazolyl moieties do not provide as good an encapsulation around the Zn–OH unites as those of the pyrazolyl moieties.

X-ray structure of complex **3**

Zinc(II) complex **3** crystallizes in a triclinic crystal system in the space group *P-1*. An ORTEP representation of the molecular structure is shown in Fig. 1 with selected bond lengths and angles contained in Table 4. The structure determination of complex **3** revealed that the zinc ion is coordinated to three thione sulfur atoms from the ligand **Tt** and one oxygen atom from the the *p*-nitrophenolate in a tetrahedral Zn[S$_3$O] arrangement with slight compression S–Zn–S angle to 107(11)°. The O1–Zn–S bond angle is 111.4(2)°. The averaged a Zn–S bond length of 2.337(3) Å and the Zn–O1 bond length of 1.951(7) Å. In complex **3**,

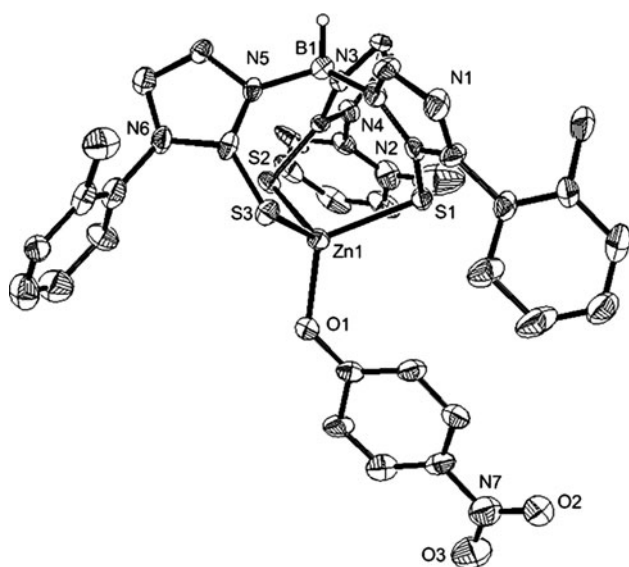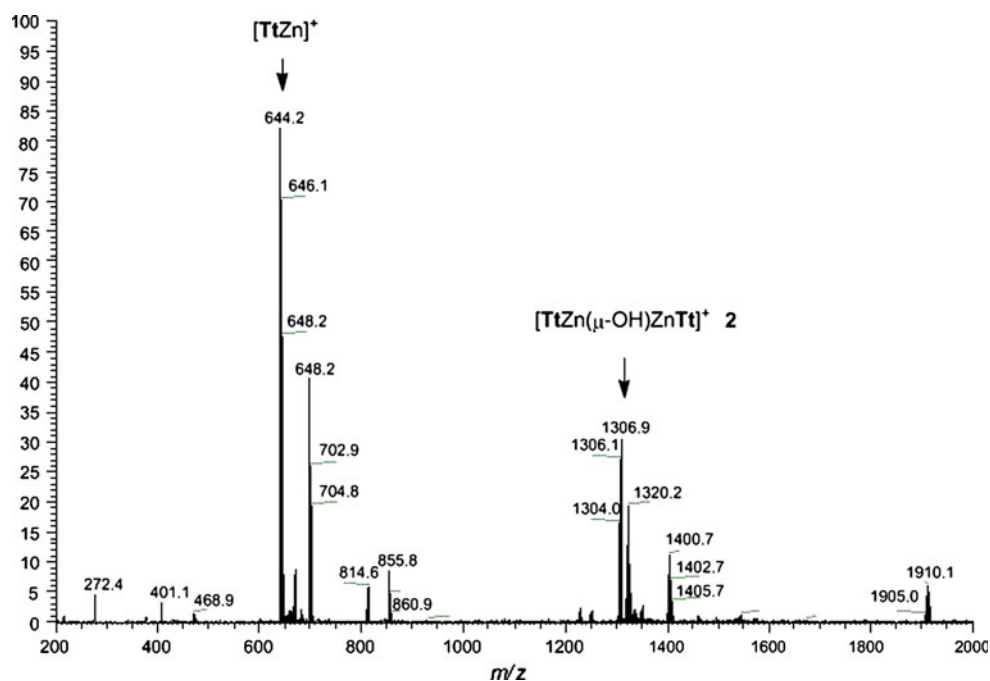**Fig. 4** ESI-Mass spectrum of the bridged hydroxo complex **2**

Fig. 5 ORTEP drawing of molecular structure of **3**. Ellipsoids are depicted at 30% probability level

Fig. 6 Packing drawing of molecular structure of **3**. Ellipsoids are depicted at 30% probability level

the ligand molecules have their S(1)C(3)N(1)N(2) moieties essentially planar and have similar bond distances: S(1)–C(3) 1.693(10) Å, N(1)–C(3) 1.344(12) Å, and N(2)–C(3) 1.372(12) Å. The bond distances reported for the free imidazolinethiole molecule are d(S–C): 1.677(4) Å, d(N–C): 1.330(3) and 1.329(4) Å [8–17]. On average, the C=S distance is increased from 1.677 Å, in the free ligand to 1.693 Å in complex **1**. This is consistent with a partial reduction of π-character of the C=S bonds in the coordinated ligands and thus a decrease of the C=S distance
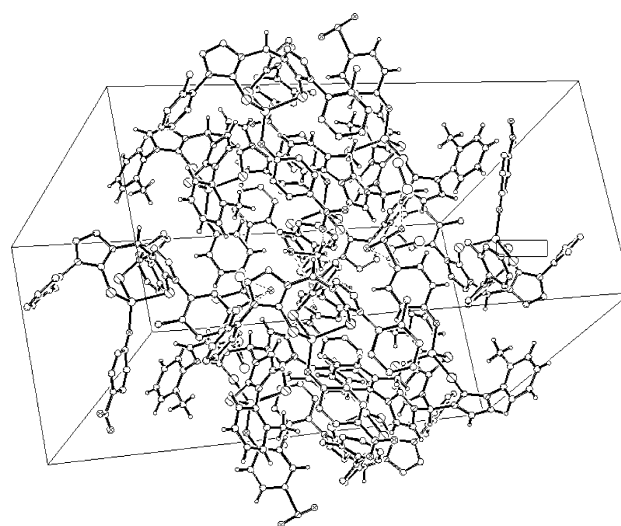
relative to the main free ligand distance [13]. This indicates that the C=S bonds are double bonds, as in the free ligand. The p-nitrophenyl ring was found to be disordered on three positions with 0.5 occupancy each. A view of the packing of **3** is shown in Fig. 3 illustrating the π···π interactions between phenyl rings (Figs. 4, 5 and 6).

The catalytic hydration of *p*-nitrophenyl acetate

In non-aqueous media, the nucleophilicity of the bridged zinc hydroxide complex **2** has been investigated for the
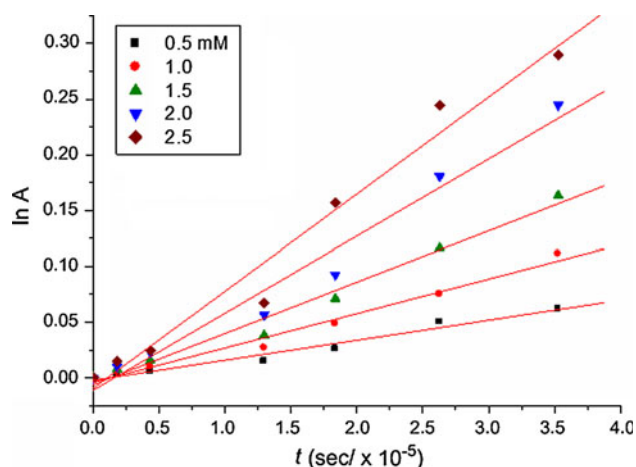
Fig. 7 Plot of the k_{obs} values for the hydrolysis of NA at various concentration of **2** (0.5–2.5 mM) in CHCl$_3$ at 300 K. Semilogarithmic plot for the cleavage of NA (8.0×10^{-5} M) at different concentrations of **2** (0.5–2.5 mM) in CHCl$_3$ at 300 K

Scheme 1 The structure of the ligand **KTt**, zinc(II) complex **1**, zinc(II) complex **2**, and the substrate *p*-nitrophenyl acetate
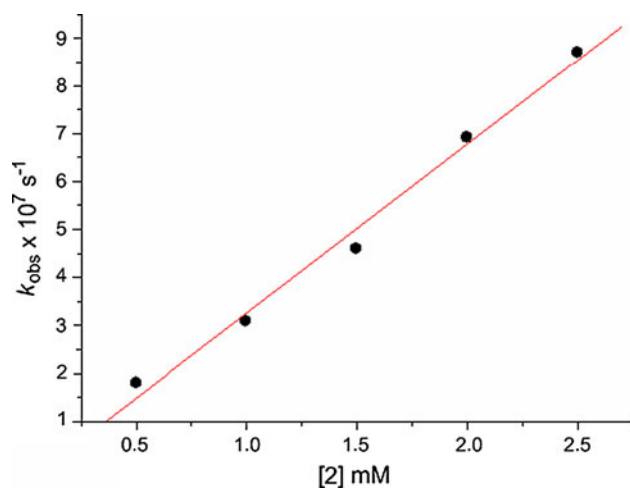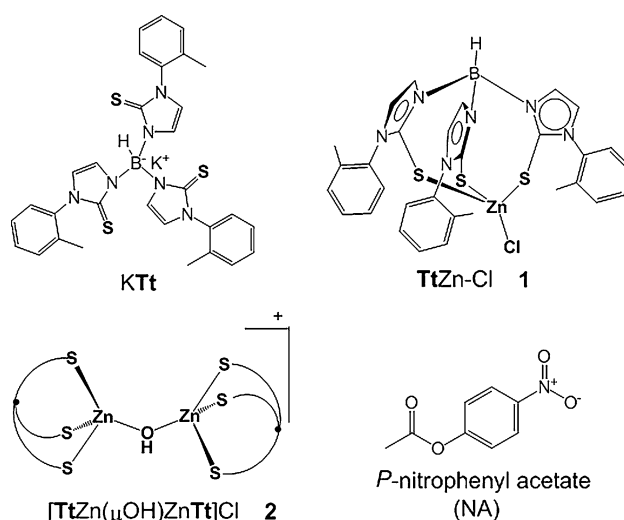

Fig. 8 Plot of the k_{obs} values for the hydrolysis of NA at various concentrations of **2** (0.5–2.5 mM) in CHCl$_3$ at 300 K

cleavage of *p*-nitrophenyl acetate, NA (Scheme 2). Its effect of catalysis was hampered by product inhibition, i.e. the phenolate, ended up in stable **TtZn–phenolate** complex **3**. So under pseudo-first order condition, by treating the NA with large excess of **2** in chloroform at 300 K, the cleaved products *p*-nitrophenolate (NP$^-$) become zinc-bound complex **3**. The four-centred mechanism established for such hydrolytic cleavage, proved that the bound NP$^-$ is the primary cleaved product without liberation of anionic NP$^-$. This was favourable for obtaining the kinetic data by recording the absorbance of **3** at 384 nm. The values of pseudo-first-order rate constants, k_{obs} were obtained from the slopes of the plots of ln($A - A_\infty$) versus time (Fig. 7). Plots of k_{obs} versus five different concentrations of **2** (Fig. 8) were linear, confirming
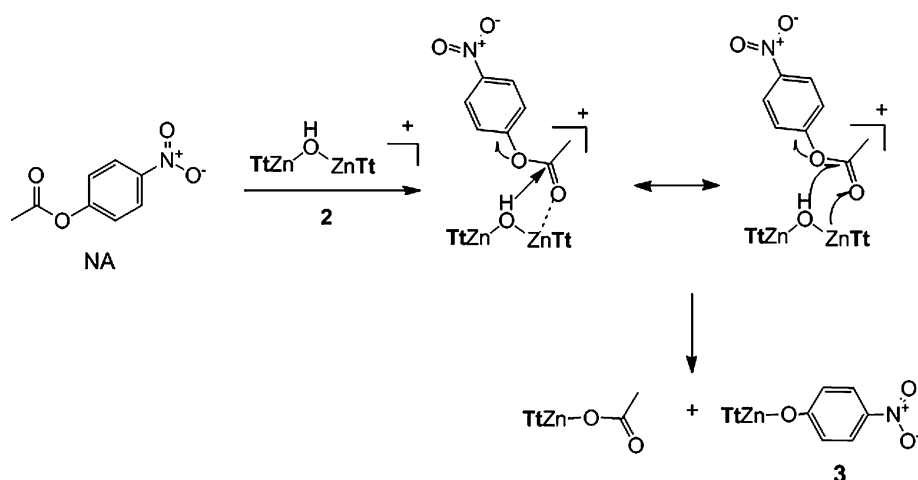
the first order dependence on [**2**]. The second-order rate constant, obtained according to $k_{obs} = k_2$ [**2**], is 3.529×10^{-4} M^{-1} s^{-1}. The plot shows that the hydrolysis reaction increases with increase in the concentration of Zn–OH$^-$ entity. This result indicates that **2** can act as a nucleophile for NA hydrolysis, taking into account that the solvent of the reactions is nonpolar (Scheme 1).

Complex **2** was found to be much less hydrolytically effective in comparison to its dimeric N$_3$-coordinated analogues [40]. This can be explained by the fact that the nitrogen donors increase the nucleophilicity of Zn–OH unit to more extent as expected from comparison with other model complexes (Tables 3, 4).

The cooperativity between the two zinc centers in **2** has been explained by a mechanism (Scheme 2) where in the intermediate the substrate and OH$^-$ are simultaneously coordinated (either on the same or two closely spaced zinc ions). The OH$^-$ acting as the nucleophile attacking the positive carbon center of the carboxy ester substrate [41]. The binding of the hydrolyzed product NP$^-$ prevents to form the nucleophilic species Zn–OH and similarly, the nucleophile species OH$^-$ cannot be exchanged with the NP$^-$. The bound NP$^-$ cannot be attacked by internal nucleophile (i.e., the formation of active Zn–OH rebels all NP$^-$ from the coordination sphere of zinc centers), so when the active species are formed, all substrates are already released. The best design would be to have two water molecules bound in the complex, and the Zn$_2$(H$_2$O)(OH) species would be the active one [42]. These results provide a conclusion that the hydrolytic efficiency of a zinc ion in N$_3$ environment is much more reactive than that found in S$_3$ environment, which is not structural model for the active site in zinc-containing hydrolase.

Scheme 2 The proposed mechanism for the hydrolytic cleavage of NA by using complex **2**

Conclusion

In this study, we have shown that the trithione containing ligand hydrotris(N-(2-methylphenyl)-2-thioimidazol-1-yl)borate, **Tt** reacts with zinc(II) chloride to form the chloro complex [**Tt**Zn–Cl] **1**. The bridged hydroxo complex [**Tt**Zn–(μ-OH)$_2$Zn**Tt**]Cl was obtained and its application towards the hydrolysis of *p*-nitrophenyl acetate was inhibited due to the formation of the stable phenolate complex [**Tt**Zn–O–Ar–*p*-NO$_2$] **3**.

Supplementary material

X-ray crystal data of **3** in CIF format are deposited with the Cambridge Crystallographic Data Centre and is available upon request. Additional supporting Figures and Tables are available from the authors upon request.

References

1. Kimura, E.: Macrocyclic polymeric zinc(II) complexes as advanced models for zinc(II) enzymes. Prog. Inorg. Chem. **41**, 443–491 (1994)
2. Vahrenkamp, H.: Transitions, transition states, transition state analogues: zinc pyrazolylborate chemistry related to zinc enzymes. Acc. Chem. Res. **32**, 589–596 (1999)
3. Kimur, E.: Model studies for molecular recognition of carbonic anhydrase and carboxypeptidase. Acc. Chem. Res. **34**, 171–179 (2001)
4. Aoki, S., Kimura, E.: Recent progress in artificial receptors for phosphate anions in aqueous solution. Rev. Mol. Biotechnol. **90**, 129–155 (2002)
5. Parkin, G.: Synthetic analogues relevant to the structure and function of zinc enzymes. Chem. Rev. **104**, 699–767 (2004)
6. Gross, F., Vahrenkamp, H.: Zinc complex chemistry of N, N, O ligands providing a hydrophobic cavity. Inorg. Chem. **44**, 3321–3329 (2005)
7. Ibrahim, M.M, Shu, M., Vahrenkamp, H.: New tris(thioimidazolyl)borate ligands and some zinc complexes thereof. Eur. J. Inorg. Chem. 1388–1397 (2005)
8. Ibrahim, M.M., He, G., Seebacher, J., Benkmil, B., Vahrenkamp, H.: Biomimetic thiolate alkylation with pyrazolyl-bis(thioimidazolyl)borate zinc complexes. Eur. J. Inorg. Chem. 4070–4077 (2005)
9. Ibrahim, M.M., Vahrenkamp, H.: Unusual formation and structure of a O-sulfinato zinc complex. Z. Anorg. Allg. Chem. 1083–1085 (2006)
10. Ibrahim, M.M., Seebacher, J., Steinfeld, G., Vahrenkamp, H.: Tris(thioimidazolyl)-borate-zinc-thiolate complexes for the modeling of biological thiolate alkylations. Inorg. Chem. **44**, 8531–8538 (2005)
11. Ibrahim, M.M.: Functionalized S$_4$Zn(II) complexes as structural modeling for the active site of thiolate-alkylating enzymes: the crystal structure of [TtiZn-SPH]$_2$·HClO$_4$ [Tti = tris(thioimidazolyl)borate and SPyH = pyridine-2-thiol]. J. Mol. Struct. **937**, 50–55 (2009)
12. Ibrahim, M.M., Shaban, S.Y.: Synthesis, characterization, and molecular structures of hydrotris(2-mercapto-1-xylyl-imidazolyl)borate-based Zn(II) and Cu(I) complexes. Inorg. Chim. Acta **362**, 1471–1477 (2009)
13. Ibrahim, M.M., Gaied, S.S., Mohsen, Q.: Synthesis and characterization of 2-mercapto-1-cyclohexylimidazole-based zinc(II) and cadmium(II) bromide complexes: the crystal structure of [Zn(Hmim^{chexyl})$_2$(Br)$_2$] with N–H···Br intermolecular hydrogen bonding interactions. Phosphorus Sulfur Silicon Relat. Elem. **185**, 2324–2332 (2009)
14. Ibrahim, M.M., Olmo, C.P., Tekeste, T., Seebacher, J., He, G., Calvo, J.A.M., Böhmerle, K., Steinfeld, G., Brombacher, H., Vahrenkamp, H.: Zn-OH$_2$ and Zn-OH complexes with hydroborate-derived tripod ligands—a comprehensive study. Inorg. Chem. **45**, 7493–7502 (2006)
15. Rombach, M., Seebacher, J., Ji, M., Zhang, G., He, G., Ibrahim, M.M., Benkmil, B., Vahrenkamp, H.: Thiolate alkylation in tripod-zinc complexes: a comparative kinetic study. Inorg. Chem. **45**, 4571–4575 (2006)
16. Shaban, S.Y., Ibrahim, M.M., Heinemann, F.W.: A new sterically loaded pentadentate N$_3$S$_2$ ligand and its zinc complexes. Inorg. Chim. Acta **360**, 2929–2934 (2007)
17. Ibrahim, M.M.: S$_4$Zn(II) complexes-containing cysteine derivatives as structural *methionine synthase* models: their catalytic

activities toward methylation reactions. J. Sulfur Chem. **31**, 394–403 (2010)

18. Lipscomb, W.N., Sträter, N.: Recent advances in zinc enzymology. Chem. Rev. **96**, 2375–2433 (1996)

19. Ibrahim, M.M., Amin, A.M., Ichikawa, K.: Synthesis and characterization of benzimidazole-based zinc complexes as structural carbonic anhydrase models and their applications towards CO_2 hydration. J. Mol. Struct. **985**, 191–201 (2011)

20. Ibrahim, M.M., Mersal, G.A.M.: Zinc(II) tweezers containing artificial peptides mimicking the active site of phosphotriesterase: the catalyzed hydrolysis of the toxic organophosphate parathion. J. Inorg. Biochem. **104**, 1195–1204 (2010)

21. Ibrahim, M.M., Ramadan, M.A.: Novel mono- and dinucleating ligands-containing artificial di- and tetrahistidine and their zinc(II) complexes as a structural *phosphotriesterase* models for the hydrolysis of *p*-nitrophenyl diphenylphosphate (*p*-NPDPP). J. Incl. Phenom. Macrocycl. Chem. **68**, 287–296 (2010)

22. Ibrahim, M.M., Eissa, H.A., Kamel, G.E., El-Baradie, H.Y.: Carbonic anhydrase inspired phosphatase model complexes derived from the tripodal ligand tris(hydroxy-2-benzimidazolyl)amine: the hydrolysis of p-nitrophenyl acetate. Synth. React. Inorg. Met.-Org. Chem. **40**, 869–878 (2010)

23. Ibrahim, M.M., Mersal, G.A.M.: Solution: chemistry of tris(2-aminoethyl)amine with metal ions of biological interest: the electroanalytical determination of the phosphate triester hydrolysis. J. Inorg. Organomet. Polym. **19**, 549–557 (2009)

24. Ibrahim, M.M.: A novel dinucleating ligand-containing hexabenzimidazoles and its dinuclear zinc complex for the hydrolysis of 2-hydroxypropyl-*p*-nitrophenyl phosphate. J. Inorg. Organomet. Polym. **19**, 532–538 (2009)

25. Ibrahim, M.M., Shaban, S.Y., Ichikawa, K.: A promising structural zinc enzyme model for CO_2 fixation and calcification. Tetrahedron Lett. **49**, 7303–7306 (2008)

26. Ibrahim, M.M.: Phosphate triester hydrolysis promoted by S_3-zinc(II) complexes with bridged hydroxide: the crystal structure of $TtiZn–OP(O)(OC_6H_4$-p-$NO_2)_2$, Tti = hydrotris(N-xylyl-2-thioimidazolyl)-borate. Inorg. Chem. Commun. **9**, 1215–1218 (2006)

27. Echizen, T., Ibrahim, M.M., Nakata, K., Izumi, M., Ichikawa, K., Shiro, M.: Nucleophilic reaction by carbonic anhydrase model zinc compound: characterization of intermediates for CO_2 hydration and phosphoester hydrolysis. J. Inorg. Biochem. **98**, 1347–1360 (2004)

28. Ibrahim, M.M., Ichikawa, K., Shiro, M.: Solution studies of N', N'', N'''-tris(3-aminopropyl)-amine-based zinc(II) complexes and X-ray crystal structures of [Zn(trpn)](ClO_4)_2 and [Zn(trpn)-(DETP)]ClO_4, DETP = *O,O*-diethyl thiophospate. Catalytic activity of the complexes in the hydrolysis of the phosphotriester 2,4-dinitrophenyl diethyl phosphate. Inorg. Chim. Acta **353**, 187–196 (2003)

29. Ibrahim, M.M.: Structural characterization of ({[tren]-Zn(HOMe)}·ClO_4 BPh_4)(tren = tris(2-aminoethyl)amine) and CO_2 fixation into monomethyl carbonato zinc(II) complex. Inorg. Chem. Commun. **6**, 1030–1034 (2003)

30. Ibrahim, M.M., Shimomura, N., Ichikawa, K., Shiro, M.: Phosphoester hydrolysis using structural phosphatase models of tren based zinc(II) complexes and crystal structures of [Zn(tren)-H_2O](ClO_4)_2 and [Zn(tren)BNPP]ClO_4. Inorg. Chim. Acta **313**, 125–136 (2001)

31. Ichikawa, K., Nakata, K., Ibrahim, M.M.: CO_2-encapsulated chlathrate hydrate formed by sulfonate assisting hydrogen bonds and template contribution from helper species of zinc(II). Chem. Lett. 796–797 (2000)

32. Ichikawa, K., Nakata, K., Ibrahim, M.M., Kawabata, S.: Biochemical CO_2 fixation by mimicking zinc(II) complex for active site of carbonic anhydrase. Adv. Surf. Sci. Catal. **114**, 309–314 (1998)

33. SAINT, V6.02, Bruker AXS, Madison, WI (1999)

34. Sheldrick, G.M.: SADABS, Area-Detector Absorption Correction, Göttingen (1996)

35. Sheldrick, G.M.: Program SHELXS, Program for Crystal Structure Determination, Göttingen (1997)

36. Temer, M., Shu, M., Vahrenkamp, H.: Sulfur-rich zinc chemistry: new tris(thioimidazolyl)hydroborate ligands and their zinc complex chemistry related to the structure and function of alcoholdehydrogenase. Inorg. Chem. **40**, 4022–4029 (2001)

37. Alsfasser, R., Trofiminko, S., Looney, A., Parkin, G., Vahrenkamp, H.: A mononuclear zinc hydroxide complex stabilized by a highly substituted tris(pyrazolyl)hydroborato ligand: analogies with the enzyme carbonic anhydrase. Inorg. Chem. **36**, 4098–4100 (1991)

38. Looney, A., Parkin, G., Ruf, M., Vahrenkamp, H.: Pyrazolylboratozink-Komplexe mit Bezug zur biologischen Funktion der Carboanhydrase. Angew. Chem. Int. Ed. Engl. **31**, 92–93 (1992)

39. Alsfasser, R., Ruf, M., Trofiminko, S., Vahrenkamp, H.: Ein L^3ZnOH-Komplex als funktionelles Modell des Enzyms Carboanhydrase. Chem. Ber. **126**, 703–710 (1993)

40. Olmo, C.P., Bohmerle, K., Vahrenkamp, H.: Zinc enzyme modelling with zinc complexes of polar pyrazolylborate ligands. Inorg. Chim. Acta **360**, 1510–1516 (2007)

41. Chang, S., Karambelkar, V.V., Sommer, R.D., Rheingold, A.L., Goldberg, D.P.: New monomeric cobalt(II) and zinc(II) complexes of a mixed N, S(alkylthiolate) ligand: model complexes of (His)(His)(Cys) metalloprotein active sites. Inorg. Chem. **41**, 239–248 (2002)

42. Hammes, B., Luo, S.X., Carrano, M.W., Carrano, C.J.: Zinc complexes of hydrogen bond accepting ester substituted trispyrazolylborates. Inorg. Chim. Acta **337**, 33–38 (2002)